Mulberroside A attenuates H_2O_2-induced oxidative stress and barrier dysfunction in Caco-2 cells through Nrf2/HO-1-associated antioxidant signaling

JIANXIN CHEN, XIUFENG HUANG, XI CHEN, WENHAI JIN and DAWEI LIN

Second Department of Gastrointestinal Surgery, Affiliated Hospital of Putian University, Putian, Fujian 351100, P.R. China

Received March 2, 2026; Accepted June 5, 2026

DOI: 10.3892/mmr.2026.13946

Abstract. Within the present study, the aim was to investigate the impact of mulberroside A on hydrogen peroxide (H_2O_2)-induced oxidative stress and intestinal epithelial barrier dysfunction, as well as explore the involvement of nuclear factor erythroid 2-related factor 2 (Nrf2)-associated antioxidant signaling. Caco-2 cells were exposed to H_2O_2 to establish an *in vitro* oxidative stress model. Cell viability, intracellular reactive oxygen species, lipid peroxidation, antioxidant enzyme activity, transepithelial electrical resistance and tight junction protein expression were assessed. Nrf2/heme oxygenase-1 (HO-1) pathway activation was evaluated using western blotting analysis and Nrf2 knockdown was used to examine pathway involvement. Results indicated that mulberroside A reduced oxidative stress levels, improved epithelial barrier function, promoted Nrf2 nuclear translocation and increased both HO-1 and NADPH quinone dehydrogenase 1 expression. These effects were attenuated following Nrf2 silencing. Overall, mulberroside A alleviated oxidative injury-associated intestinal epithelial barrier dysfunction in Caco-2 cells, supporting its potential relevance in oxidative stress-associated intestinal disorders.

Introduction

As a key component in maintaining gut homeostasis, the intestinal epithelial barrier permits selective nutrient uptake while preventing the infiltration of luminal pathogens, toxins and antigens. The functional integrity of this barrier relies on epithelial cell viability, the proper organization of tight junction proteins and the maintenance of intracellular redox balance. Epidemiological evidence indicates that inflammatory bowel disease affects ~4.9 million individuals globally, with a steadily increasing incidence and prevalence over recent decades across both high-income and newly industrialized regions (1,2). Disruption of epithelial barrier integrity is widely recognized as a key pathological feature in numerous gastrointestinal disorders, including inflammatory bowel disease and oxidative stress-associated mucosal injury (3,4). Among the pathogenic mechanisms involved, oxidative stress serves as a key contributor to epithelial dysfunction. Excessive accumulation of reactive oxygen species (ROS) can directly damage cellular macromolecules, compromise tight junction architecture and amplify inflammatory responses, ultimately leading to barrier breakdown (5,6). Although oxidative stress has been increasingly acknowledged as an important therapeutic target (3,7), effective strategies that directly protect intestinal epithelial cells against oxidative stress-mediated barrier impairment remain limited. Several antioxidants, phytochemicals and microbiota-targeted interventions have demonstrated protective effects in experimental models (8,9); however, their clinical translation remains constrained by poor bioavailability, insufficient target specificity and limited robust evidence from human studies (10,11).

Nuclear factor erythroid 2-related factor 2 (Nrf2) functions as a central regulator of cellular antioxidant defense and redox homeostasis. Upon oxidative challenge, Nrf2 undergoes nuclear translocation, where it activates the transcription of numerous cytoprotective genes, including heme oxygenase-1 (HO-1) and NADPH quinone dehydrogenase 1 (NQO1). Increasing evidence over the past decade has indicated that Nrf2 pathway activation not only alleviates oxidative damage, but also contributes to the preservation of epithelial integrity, modulation of inflammatory responses and maintenance of gastrointestinal barrier function (12,13). Concurrently, bioactive compounds derived from natural sources have garnered marked attention as modulators of oxidative stress due to their favorable safety profiles and multitarget biological activities. Numerous studies have demonstrated that plant-derived polyphenols and glycosides can attenuate intestinal oxidative stress and improve epithelial barrier function through regulation of Nrf2-dependent antioxidant pathways (14,15).

Mulberroside A is a naturally occurring stilbene glycoside isolated from *Morus* species and has been reported to exhibit a

Correspondence to: Dr Xiufeng Huang or Dr Xi Chen, Second Department of Gastrointestinal Surgery, Affiliated Hospital of Putian University, 999 Dongzhen East Road, Licheng, Putian, Fujian 351100, P.R. China
E-mail: cjxptyy@126.com
E-mail: watermelons0224@163.com

Key words: mulberroside A, oxidative stress, intestinal epithelial barrier, nuclear factor erythroid 2-related factor 2, tight junction proteins

broad spectrum of pharmacological properties, including antioxidant and anti-inflammatory effects (16). Previous studies have shown that mulberroside A may effectively reduce oxidative stress and confer cytoprotection in cardiovascular, hepatic and neural cell models (17-19). Emerging evidence has further suggested that this compound may influence redox-sensitive signaling pathways and antioxidant enzyme expression, implying its potential regulatory effect upon Nrf2-associated mechanisms. However, to the best of our knowledge, despite these findings, the role of mulberroside A in intestinal epithelial oxidative stress has not been systematically explored (12). In particular, its effects on oxidative stress-induced intestinal barrier impairment and tight junction integrity, as well as the associated molecular mechanisms, remain largely undefined.

Therefore, the present study evaluated the protective actions of mulberroside A on hydrogen peroxide (H_2O_2)-evoked oxidative stress and barrier dysfunction using Caco-2 intestinal epithelial cells. Its impact on oxidative stress parameters, epithelial barrier integrity and activation of the Nrf2-mediated antioxidant response were examined. In addition, Nrf2 gene silencing was employed to clarify the mechanistic contribution of Nrf2 signaling to the protective actions of mulberroside A.

Materials and methods

Cell culture and reagents. Caco-2, the human colorectal adenocarcinoma cell line, was obtained from the American Type Culture Collection (cat. no. ATCC-HTB-37). Cell line authentication was provided by the supplier and routine testing determined that the cells were *Mycoplasma*-free. Mulberroside A (purity ≥98%) was purchased from MedChemExpress (cat. no. HY-N0619). Mulberroside A was dissolved in DMSO to prepare a stock solution and subsequently diluted with culture medium to the indicated working concentrations. The final DMSO concentration in all treatment groups was maintained <0.1% (v/v). Caco-2 cells were cultured in DMEM containing 10% FBS and 1% penicillin-streptomycin. Cells were maintained at 37˚C in 5% CO_2. The medium was changed every 2-3 days and cells at the logarithmic growth stage were selected for subsequent experiments. All experiments were performed using Caco-2 cells between passages 20-35 to ensure the formation of a physiological intestinal epithelial barrier with transepithelial electrical resistance values >50 Ωcm^2, consistent with previously established criteria for barrier-competent Caco-2 monolayers (20).

Establishment of oxidative stress model and experimental grouping. To establish an *in vitro* model of oxidative stress-mediated intestinal epithelial damage, Caco-2 cells were treated with H_2O_2, which is commonly used to induce acute oxidative damage in intestinal epithelial cells (21). H_2O_2 was administered at 500 μM (final concentration), a condition selected based on previous studies and preliminary experiments (22).

To assess the effects of mulberroside A, cells were initially treated with increasing concentrations of mulberroside A (0, 5, 10, 20 and 40 μM) at 37˚C for 24 h to evaluate cellular responses. Based on the dose-screening results, three concentrations, 5 μM (low), 10 μM (medium) and 20 μM (high), were selected for subsequent experiments.

For functional and mechanistic analyses, cells were assigned to the following groups: i) Control; ii) H_2O_2; and iii) H_2O_2 combined with mulberroside A (5, 10 or 20 μM). In the mulberroside A treatment groups, cells were pretreated with mulberroside A at 37˚C for 30 min, followed by exposure to 500 μM H_2O_2 for 6 h at 37˚C in the continued presence of mulberroside A. To further determine the involvement of Nrf2 signaling, additional groups were established in which cells were transfected with Nrf2-specific small interfering RNA (siNrf2) or negative control siRNA (siNC) prior to mulberroside A pretreatment and H_2O_2 exposure. Subsequently, two independent siRNA sequences targeting Nrf2 were initially evaluated for knockdown efficiency and the sequence exhibiting higher efficiency was selected for further functional experiments.

siRNA transfection. siRNAs targeting human Nrf2 and a corresponding negative control siRNA were commercially synthesized by GenePharma Co., Ltd. Transient siRNA transfection was carried out in Caco-2 cells using Lipofectamine™ RNAiMAX Transfection Reagent (cat. no. 13778075; Thermo Fisher Scientific, Inc.) according to the manufacturer's instructions. Briefly, cells were transfected with siRNAs at a final concentration of 50 nM and incubated at 37˚C in a humidified atmosphere containing 5% CO_2 for 48 h to achieve effective knockdown of Nrf2 expression before subsequent treatments. The efficiency of Nrf2 silencing was verified at the mRNA level by reverse transcription-quantitative PCR (RT-qPCR) using GAPDH as the internal control prior to functional and molecular analyses. The detailed sequences of the siRNAs used are provided in Table SI.

Cell viability assay. Caco-2 cells were plated in 96-well plates and exposed to the designated treatments. After treatment, CCK-8 reagent (cat. no. CK04; Dojindo Molecular Technologies, Inc.) was added to each well at a final concentration of 10% (v/v) and cells were incubated under standard culture conditions for 2 h. Absorbance at 450 nm was recorded with a microplate spectrophotometer (SpectraMax® iD3; Molecular Devices, LLC.). Cell viability was calculated as a percentage of the control group.

Determination of intracellular ROS. ROS levels were assessed with a fluorescent ROS detection kit based on 2',7'-dichlorofluorescein diacetate (cat. no. S0033S; Beyotime Biotechnology). Following the indicated treatments, Caco-2 cells were incubated with the fluorescent probe at 37˚C for 30 min under light-protected conditions, followed by fluorescence microscopy. The fluorescence signal was analyzed as integrated density using ImageJ software (version 1.53c; National Institutes of Health). ROS levels were quantified as relative integrated fluorescence values, and the results were normalized to the control group.

Transepithelial electrical resistance (TEER) measurement. Intestinal epithelial barrier integrity was assessed by TEER. Caco-2 cells were seeded onto Corning® Transwell® inserts (cat. no. 3413; Corning, Inc.) to form confluent monolayers. TEER values were measured using an EVOM2 epithelial volt/ohm meter with STX2 electrodes (World Precision

Instruments), corrected by subtracting blank insert resistance and normalized to the membrane surface area.

Western blotting. Using a nuclear/cytoplasmic protein extraction kit (cat. no. P0027; Beyotime Biotechnology), nuclear and cytoplasmic fractions were prepared and protein concentrations were quantified using a Pierce™ BCA assay kit (cat. no. 23227; Thermo Fisher Scientific, Inc.). After 30 μg of protein per sample was separated by SDS-PAGE and transferred to PVDF membranes (cat. no. IPVH00010; MilliporeSigma; Merck KGaA). Membranes were blocked with 5% non-fat milk (Beyotime Biotechnology) at room temperature for 60 min. Subsequently, membranes were incubated overnight at 4˚C with the following primary antibodies: Nrf2 (cat. no. ab62352; 1:1,000; Abcam), HO-1 (cat. no. ab189491; 1:2,000; Abcam), NQO1 (cat. no. ab80588; 1:10,000; Abcam), lamin B1 (cat. no. 12987-1-AP; 1:5,000; Proteintech Group, Inc.) and GAPDH (cat. no. 81640-5-RR; 1:10,000; Proteintech Group, Inc.). After washing three times with TBST (10 min each), membranes were incubated with HRP-conjugated secondary antibodies at room temperature for 60 min: Goat anti-rabbit IgG H&L/HRP (bs-0295G-HRP; 1:3,000; BIOSS) or goat anti-mouse IgG H&L/HRP (bs-0296G-HRP; 1:3,000; BIOSS), depending on the primary antibody host species. Signals were developed using Pierce™ ECL reagent (cat. no. 32106; Thermo Fisher Scientific, Inc.) and densitometry analysis was performed using ImageJ software (version 1.53c; National Institutes of Health).

RT-qPCR. Total RNA was extracted from Caco-2 cells using TRIzol™ reagent (cat. no. 15596026; Thermo Fisher Scientific, Inc.). Complementary DNA was synthesized using the PrimeScript™ reverse transcription kit (cat. no. RR037A; Takara Bio, Inc.) according to the manufacturer's instructions, with a reverse transcription reaction at 37˚C for 15 min followed by enzyme inactivation at 85˚C for 5 sec. Using SYBR Green Master Mix (cat. no. RR420A; Takara Bio, Inc.), quantitative real-time PCR was conducted on a QuantStudio 5 real-time PCR system (Applied Biosystems). The thermocycling conditions were as follows: Initial denaturation at 95˚C for 30 sec, followed by 40 cycles of denaturation at 95˚C for 5 sec and annealing/extension at 60˚C for 30 sec. A melt curve analysis was subsequently performed to verify amplification specificity. Relative mRNA expression was determined using the $2^{-\Delta\Delta Cq}$ method (23) with GAPDH as the internal control. The primer used sequences were as follows: Nrf2 forward, 5'-ACAAACATTCAAGCC GCTTGG-3' and reverse, 5'-CGTAGCATGCTGAAAACT TCG-3'; GAPDH forward, 5'-AAGATCATCAGCAATGCC TCC-3' and reverse, 5'-AGGTTTTTCTAGACGGCAGG-3'.

Measurement of malondialdehyde (MDA) and superoxide dismutase (SOD) levels. Following the indicated treatments, Caco-2 cells were lysed using Cell Lysis Buffer (cat. no. P0013; Beyotime Biotechnology) according to the manufacturer's instructions. Cell lysates were collected and used for the determination of lipid peroxidation and antioxidant capacity by measuring MDA content and total SOD activity using a Lipid Peroxidation (MDA) Assay Kit (cat. no. S0131S; Beyotime Biotechnology) and a Total SOD Activity Assay Kit (cat. no. S0101S; Beyotime Biotechnology), respectively, according to the manufacturers' protocols. Absorbance was recorded spectrophotometrically using a SpectraMax® iD3 microplate reader (Molecular Devices, LLC.) and MDA and SOD values were normalized to total protein concentration.

Immunofluorescence staining. After treatment, Caco-2 cells cultured on glass coverslips were fixed with 4% paraformaldehyde at room temperature for 20 min, permeabilized and blocked with 5% bovine serum albumin (cat. no. ST025; Beyotime Biotechnology) at room temperature for 30 min. Immunofluorescence staining was subsequently performed to assess the expression and localization of tight junction proteins. Cells were then incubated with primary antibodies against zonula occludens 1 (ZO-1; cat. no. ab96587; 1:200; Abcam) and occludin (cat. no. ab216327; 1:200; Abcam) at 4˚C overnight. After washing with PBS, cells were incubated with Alexa Fluor™ 488-conjugated goat anti-rabbit IgG (H+L) secondary antibody (cat. no. A-11008; 1:500; Thermo Fisher Scientific, Inc.) at room temperature for 1 h in the dark. Nuclei were counterstained with DAPI (cat. no. D9542; Sigma-Aldrich; Merck KGaA) at room temperature for 10 min. Fluorescence images were acquired using the IX73 fluorescence microscope (Olympus Corporation).

Statistical analysis. Each experiment was independently repeated at least three times. Data are reported as the mean ± SD. Statistical analyses were conducted using SPSS software (version 26.0; IBM Corp.). Differences among multiple groups were analyzed using one-way ANOVA tests followed by Tukey's post hoc test. $P<0.05$ was considered to indicate a statistically significant difference.

Results

Impact of mulberroside A on Caco-2 cell viability. Fig. 1A shows the chemical structure of mulberroside A, which was obtained from the ChEMBL database (https://www.ebi.ac.uk/chembl/). Mulberroside A is a stilbene glycoside composed of a central stilbene backbone bearing numerous phenolic hydroxyl groups and glycosidic moieties. Based on the CCK-8 assay, treatment of Caco-2 cells with 5 μM mulberroside A for 24 h did not significantly affect cell viability compared with the 0 μM (control) group ($P>0.05$; Fig. 1B). By contrast, treatment with 10 μM mulberroside A significantly decreased cell viability compared with the control group ($P<0.05$). A further decline in viability was observed in the 20 μM mulberroside A-treated group ($P<0.001$ vs. 0 μM), whereas treatment with 40 μM mulberroside A resulted in a more pronounced reduction ($P<0.001$ vs. 0 μM). These findings suggested that mulberroside A exerted limited effects on basal Caco-2 cell viability at 5 μM, whereas higher concentrations tended to reduce cell viability.

Effect of mulberroside A on H_2O_2-induced oxidative stress and barrier dysfunction in Caco-2 cells. As shown in Fig. 2A, H_2O_2 exposure significantly decreased Caco-2 cell viability compared with the control group ($P<0.001$). Pretreatment with mulberroside A at low, medium and high concentration significantly restored cell viability compared with the H_2O_2 group

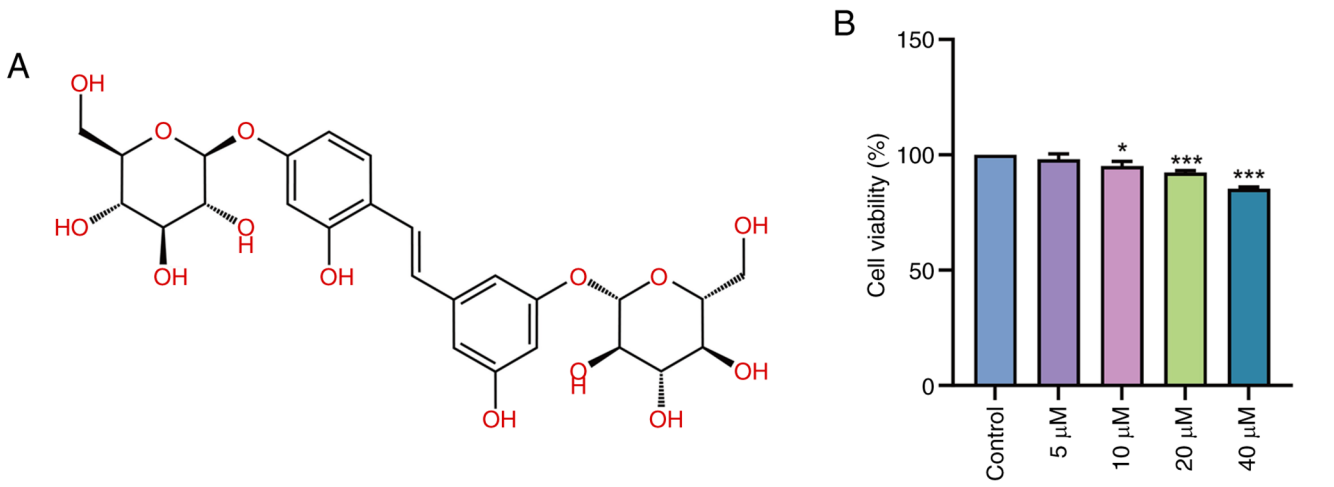

Figure 1. Effect of mulberroside A on Caco-2 cell viability. (A) Chemical structure of mulberroside A. The structural information was obtained from the ChEMBL database (https://www.ebi.ac.uk/chembl/). (B) Caco-2 cell viability after 24 h exposure to mulberroside A (0, 5, 10, 20 and 40 μM), measured using a Cell Counting Kit-8 assay. Data are presented as the mean ± SD from three independent experiments. *P<0.05 and ***P<0.001 vs. control.

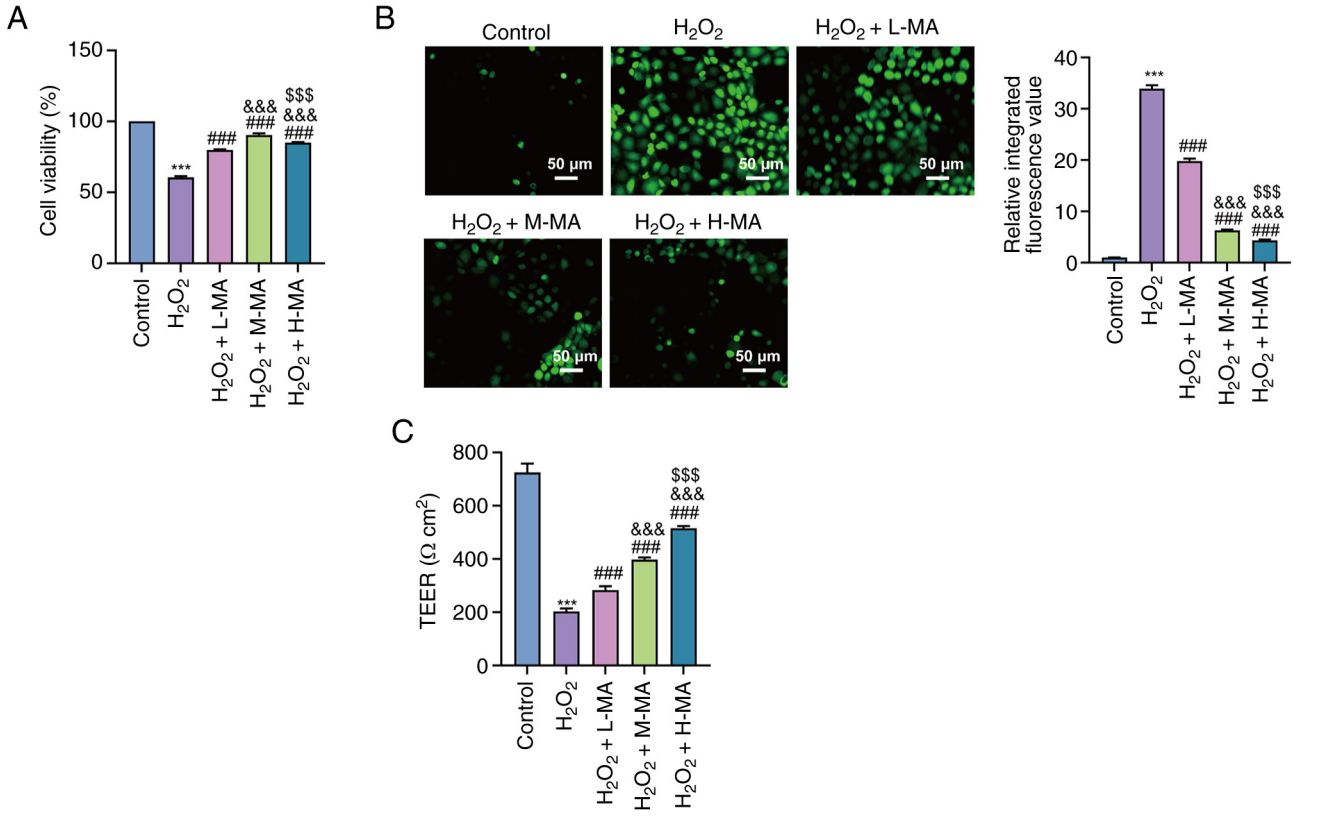

Figure 2. Effect of MA on H_2O_2-induced oxidative stress and barrier dysfunction in Caco-2 cells. (A) Cell viability of Caco-2 cells in the control, H_2O_2, H_2O_2 + L-MA (5 μM), H_2O_2 + M-MA (10 μM) and H_2O_2 + H-MA (20 μM) groups, as assessed using a Cell Counting Kit-8 assay. (B) Intracellular reactive oxygen species levels (representative fluorescence images shown; scale bar, 50 μm). (C) TEER of Caco-2 cell monolayers following the indicated treatments. Data are presented as the mean ± SD from three independent experiments. ***P<0.001 vs. control, $^{###}$P<0.001 vs. H_2O_2, $^{&&&}$P<0.001 vs. H_2O_2 + L-MA and $^{$$$}$P<0.001 vs. H_2O_2 + M-MA. H_2O_2, hydrogen peroxide; MA, mulberroside A; L-MA, low-dose MA; M-MA, medium-dose MA; H-MA, high-dose MA; TEER, transepithelial electrical resistance.

(all, P<0.001). Significant differences in cell viability were observed among the mulberroside A-treated groups (P<0.001), with the medium-dose group exhibiting the greatest increase in viability.

Intracellular ROS levels were significantly increased following H_2O_2 treatment compared with the control group (P<0.001; Fig. 2B), whereas mulberroside A significantly suppressed ROS accumulation at all tested concentrations compared with the H_2O_2 group (all, P<0.001). Significant differences were also observed among the low-, medium- and high-dose mulberroside A groups (all, P<0.001), demonstrating a concentration-dependent reduction in ROS levels.

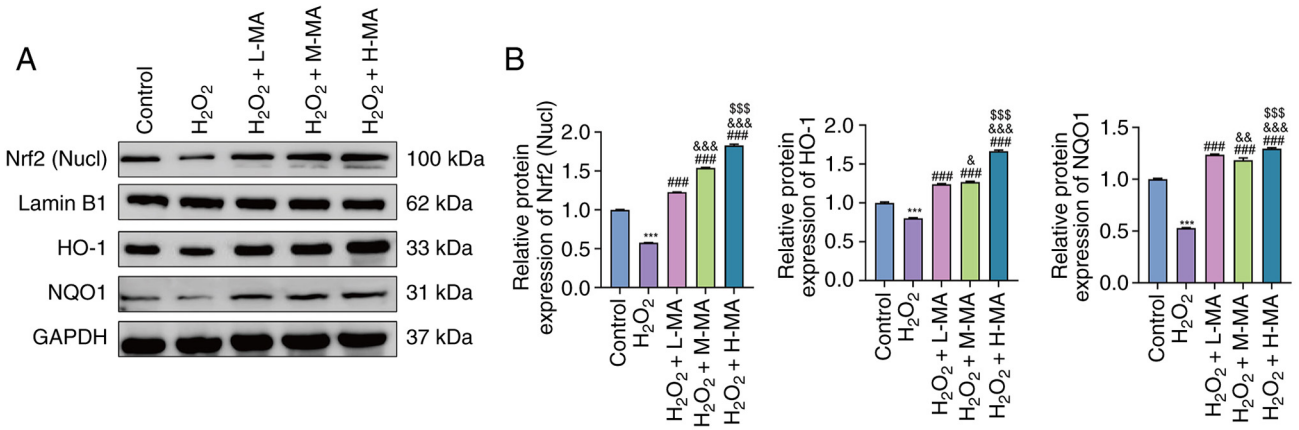

Figure 3. Effect of MA on Nrf2/HO-1/NQO1 protein expression in Caco-2 cells. (A) Representative western blotting of nucl Nrf2 and total HO-1 and NQO1 in control, H_2O_2, H_2O_2 + L-MA, H_2O_2 + M-MA and H_2O_2 + H-MA groups. (B) Densitometric quantification normalized to the corresponding internal controls. Data are presented as the mean ± SD from three independent experiments. ***P<0.001 vs. control, $^{###}$P<0.001 vs. H_2O_2, $^{&}$P<0.05 vs. H_2O_2 + L-MA, $^{&&}$P<0.01 vs. H_2O_2 + L-MA, $^{&&&}$P<0.001 vs. H_2O_2 + L-MA; and $^{$$$}$P<0.001 vs. H_2O_2 + M-MA. H_2O_2, hydrogen peroxide; MA, mulberroside A; L-MA, low-dose MA; M-MA, medium-dose MA; H-MA, high-dose MA; Nucl, nuclear; Nrf2, nuclear factor erythroid 2-related factor 2; HO-1, heme oxygenase 1; NQO1, NADPH quinone dehydrogenase 1.

H_2O_2 exposure also caused a significant reduction in TEER compared with the control group (P<0.001; Fig. 2C). Mulberroside A significantly elevated TEER values compared with the H_2O_2 group at all tested concentrations (all, P<0.001). TEER values progressively increased with increasing mulberroside A concentrations, supporting a concentration-dependent restoration of epithelial barrier integrity (P<0.001).

Effect of mulberroside A on Nrf2/HO-1/NQO1 pathway protein levels in Caco-2 cells. As shown in Fig. 3A and B, H_2O_2 treatment significantly decreased nuclear Nrf2 protein levels compared with the control group (P<0.001). Mulberroside A treatment at low, medium and high concentrations significantly increased nuclear Nrf2 levels compared with the H_2O_2 group (all, P<0.001). In addition, significant inter-dose differences were observed among the mulberroside A-treated groups (P<0.001), indicating a concentration-dependent increase in nuclear Nrf2 accumulation.

Similarly, total HO-1 protein levels were significantly reduced following H_2O_2 treatment compared with the control group (P<0.001). Mulberroside A treatment then significantly increased HO-1 protein levels compared with the H_2O_2 group (P<0.001) and HO-1 expression progressively increased with increasing mulberroside A concentrations (P<0.05).

Consistent changes were observed for NQO1 protein expression. H_2O_2 exposure significantly decreased NQO1 levels compared with the control group (P<0.001), whereas mulberroside A significantly restored NQO1 expression at all tested concentrations compared with the H_2O_2 group (all, P<0.001). Significant differences among all mulberroside A dose groups were also detected (P<0.01), further supporting a concentration-associated activation of the Nrf2/HO-1/NQO1 antioxidant pathway.

Effect of Nrf2 knockdown on mulberroside A-associated alterations in oxidative stress-associated parameters in Caco-2 cells. As depicted in Fig. 4A, reverse transcription-quantitative PCR analysis demonstrated that transfection with siNrf2#1 and siNrf2#2 significantly reduced Nrf2 mRNA levels in Caco-2 cells compared with the siNC group (P<0.001). Based on knockdown efficiency, siNrf2#2 was selected for subsequent experiments.

Western blotting further demonstrated that H_2O_2 treatment significantly reduced nuclear Nrf2 and total HO-1 and NQO1 protein levels compared with the control group (P<0.001; Fig. 4B and C). In the H_2O_2 + mulberroside A + siNC group, these proteins were significantly increased compared with the H_2O_2 group (P<0.001). By contrast, Nrf2 silencing significantly reduced nuclear Nrf2, HO-1 and NQO1 protein levels compared with the H_2O_2 + mulberroside A + siNC group (all P<0.001).

Quantification of DCF fluorescence revealed that the relative integrated fluorescence value was significantly increased following H_2O_2 exposure compared with the control group (P<0.001; Fig. 4D), whereas mulberroside A significantly reduced ROS accumulation in siNC-transfected cells compared with the H_2O_2 group (P<0.001). This inhibitory effect was significantly attenuated by Nrf2 knockdown, as indicated by higher ROS levels in the H_2O_2 + mulberroside A + siNrf2 group compared with the H_2O_2 + mulberroside A + siNC group (P<0.001).

Consistently, H_2O_2 significantly increased MDA levels and decreased SOD activity compared with the control group (both, P<0.001; Fig. 4E and F). Mulberroside A significantly reduced MDA levels, but restored SOD activity in siNC-transfected cells compared with the H_2O_2 group (both, P<0.001). However, Nrf2 knockdown significantly weakened these effects, resulting in higher MDA levels and lower SOD activity compared with the H_2O_2 + mulberroside A + siNC group (both, P<0.001).

Effect of Nrf2 knockdown on epithelial barrier integrity and tight junction protein expression in Caco-2 cells. As shown in Fig. 5A, H_2O_2 exposure significantly decreased TEER compared with the control group (P<0.001). Mulberroside A significantly restored TEER in siNC-transfected cells compared with the H_2O_2 group (P<0.001). By contrast, Nrf2 knockdown significantly reduced TEER compared with the

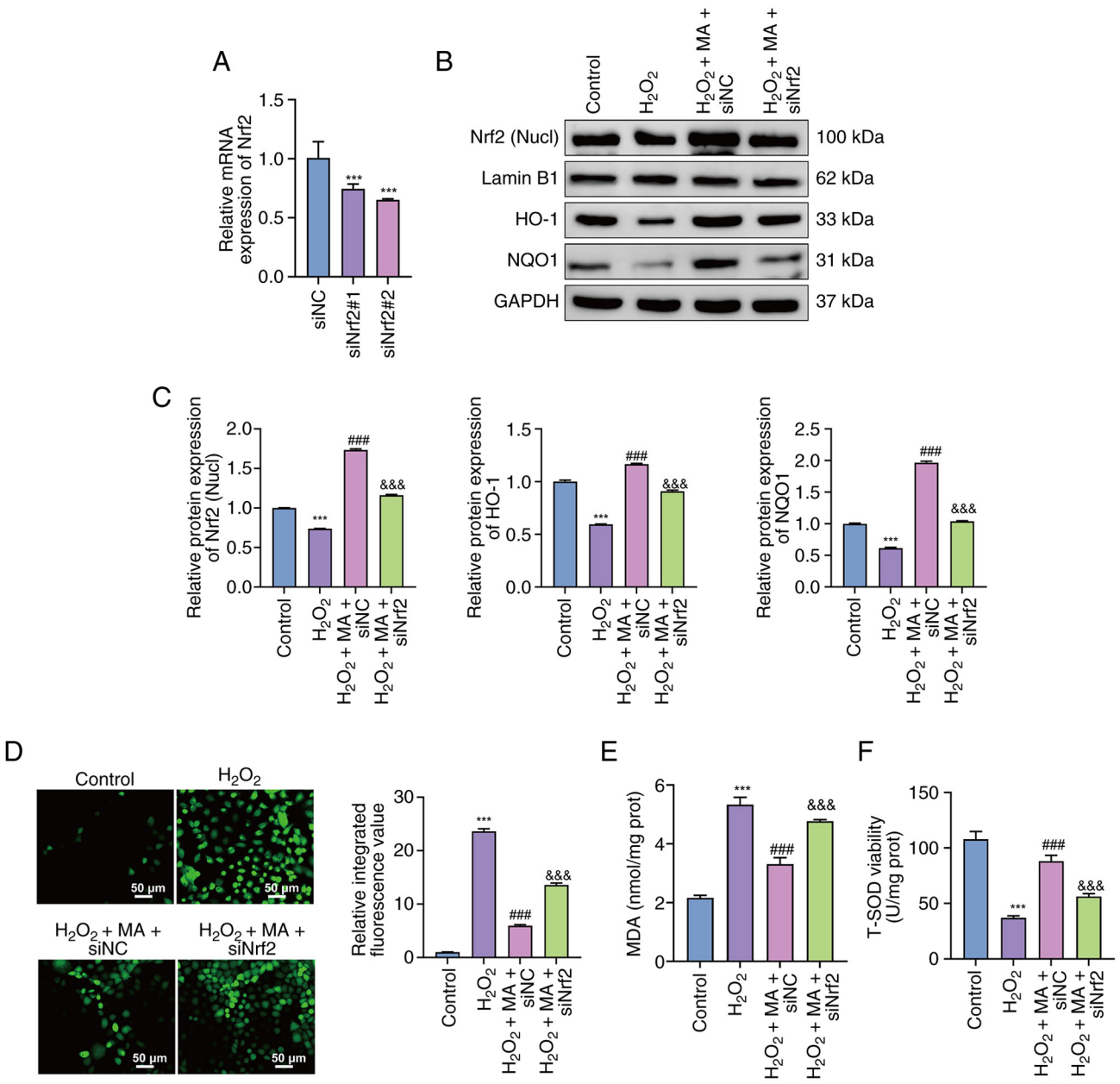

Figure 4. Impact of Nrf2 knockdown on MA-associated changes in oxidative stress-associated parameters in Caco-2 cells. (A) Nrf2 mRNA levels after transfection with siNC, siNrf2#1 or siNrf2#2, as determined by reverse transcription-quantitative PCR. ***P<0.001 vs. siNC. (B) Representative western blotting of nucl Nrf2 and total HO-1 and NQO1 in control, H_2O_2, H_2O_2 + MA + siNC and H_2O_2 + MA + siNrf2 groups. (C) Densitometric quantification normalized to internal controls. (D) Intracellular reactive oxygen species levels, quantified as relative integrated fluorescence intensity of DCF fluorescence images (representative fluorescence images; scale bar, 50 μm). (E) MDA levels. (F) SOD activity. Data are presented as the mean ± SD from three independent experiments. ***P<0.001 vs. control, ###P<0.001 vs. H_2O_2 and &&&P<0.001 vs. H_2O_2 + MA+ siNC. H_2O_2, hydrogen peroxide; MA, mulberroside A; L-MA, low-dose MA; M-MA, medium-dose MA; H-MA, high-dose MA; Nucl, nuclear; Nrf2, nuclear factor erythroid 2-related factor 2; si, small interfering RNA; NC, negative control; MDA, malondialdehyde; SOD, superoxide dismutase.

H_2O_2 + mulberroside A + siNC group (P<0.001), indicating that Nrf2 silencing attenuated the barrier-protective effect of mulberroside A.

Consistently, immunofluorescence analysis showed that H_2O_2 markedly decreased ZO-1 and occludin fluorescence intensities compared with the control group (both, P<0.001; Fig. 5B and C). Mulberroside A significantly increased both ZO-1 and occludin signals in siNC-transfected cells compared with the H_2O_2 group (both, P<0.001). However, Nrf2 knockdown significantly attenuated these increases, as reflected by lower ZO-1 and occludin fluorescence intensities in the H_2O_2 + mulberroside A + siNrf2 group compared with the H_2O_2 + mulberroside A + siNC group (both, P<0.001).

Discussion

In the present study, the impact of mulberroside A on oxidative stress-induced intestinal epithelial injury was systematically characterized using an H_2O_2-challenged Caco-2 cell model. Exposure to H_2O_2 resulted in notable oxidative injury and epithelial barrier impairment, as evidenced by increased intracellular ROS levels, reduced transepithelial electrical

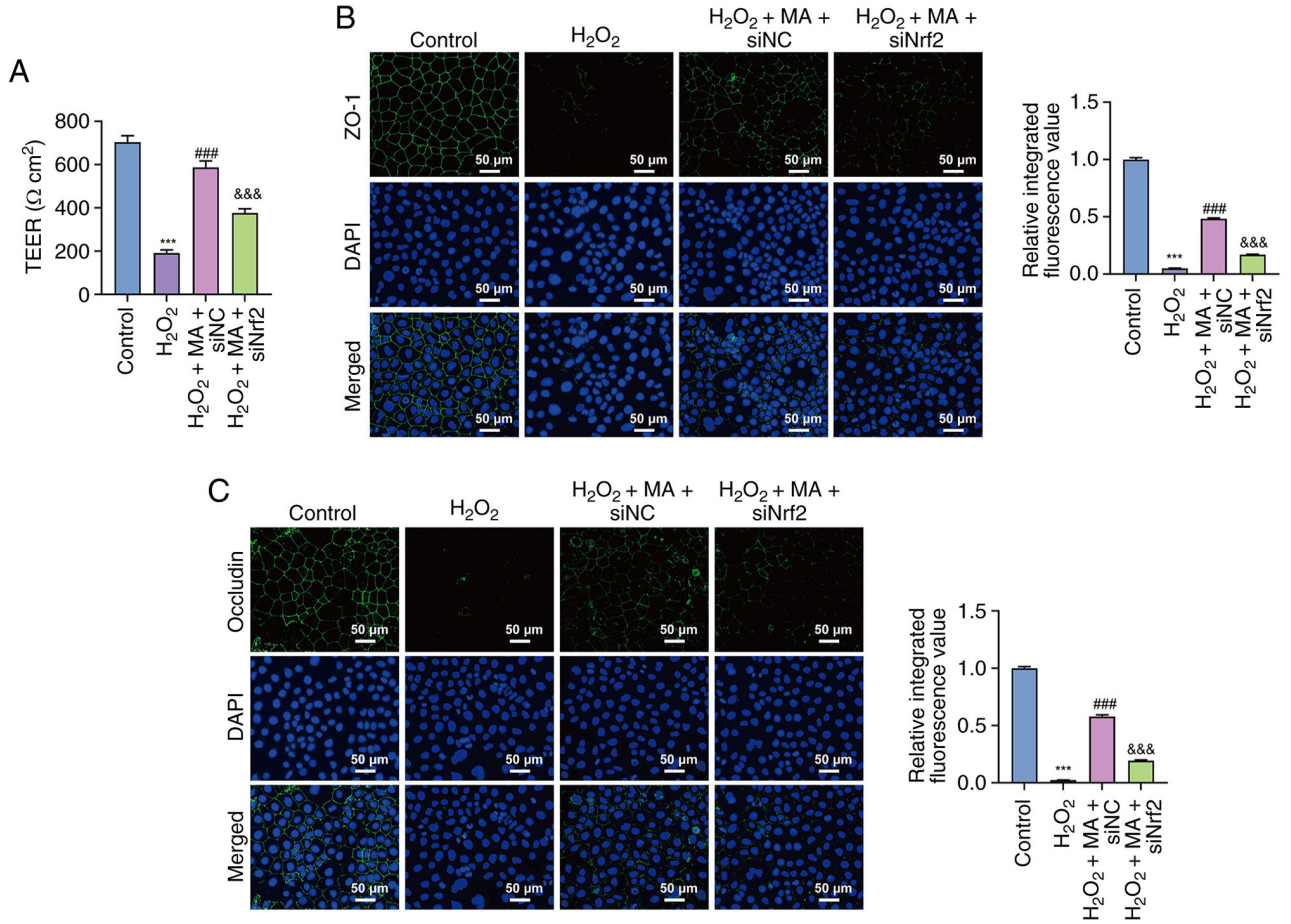

Figure 5. Effects of Nrf2 knockdown on epithelial barrier function and tight junction protein distribution in Caco-2 cells. (A) TEER in control, H_2O_2, H_2O_2 + MA + siNC and H_2O_2 + MA + siNrf2 groups. Immunofluorescence staining of (B) ZO-1 and (C) occludin. Data are presented as the mean ± SD from three independent experiments. ***P<0.001 vs. control, $^{###}$P<0.001 vs. H_2O_2 and $^{&&&}$P<0.001 vs. H_2O_2 + MA + siNC. H_2O_2, hydrogen peroxide; MA, mulberroside A; L-MA, low-dose MA; M-MA, medium-dose MA; H-MA, high-dose MA; Nucl, nuclear; Nrf2, nuclear factor erythroid 2-related factor 2; si, small interfering RNA; NC, negative control; TEER, transepithelial electrical resistance; ZO-1, zonula occludens 1.

resistance and disrupted expression of the tight junction proteins ZO-1 and occludin. Within the concentration range examined, mulberroside A markedly attenuated these alterations, accompanied by enhanced nuclear accumulation of Nrf2 and upregulated expression of the downstream antioxidant proteins HO-1 and NQO1. Notably, genetic silencing of Nrf2 markedly weakened the mulberroside A-associated changes in oxidative stress markers, barrier integrity and tight junction protein expression. Collectively, these findings revealed a coherent pattern showing an association between oxidative stress modulation, antioxidant signaling activation and epithelial barrier preservation in the context of mulberroside A treatment.

Oxidative stress is widely recognized as a central pathological driver of intestinal epithelial barrier disruption and excessive ROS production has been shown to compromise epithelial integrity by directly damaging cellular components and destabilizing tight junction architecture (22,24,25). Previous studies have demonstrated that elevated ROS levels are associated with reductions in transepithelial electrical resistance and disorganization of key tight junction proteins, including ZO-1 and occludin, ultimately leading to increased epithelial permeability (24,26). These observations are consistent with the present findings, in which H_2O_2 exposure triggered marked oxidative stress in Caco-2 cells, accompanied by notable decreases in TEER and disrupted expression of tight junction proteins. Furthermore, the coordinated recovery of ROS levels, TEER and tight junction integrity observed following mulberroside A treatment aligns with the established concept that restoration of redox homeostasis is associated with the preservation of epithelial barrier integrity (26-28).

From a molecular perspective, the Nrf2 pathway has been extensively characterized as a key regulator of cellular antioxidant defense and epithelial protection (29,30). Activation of Nrf2 promotes its nuclear translocation and subsequent transcriptional upregulation of cytoprotective enzymes, including HO-1 and NQO1, which serve key roles in mitigating oxidative injury and maintaining epithelial homeostasis. Accumulating evidence has indicated that impairment of Nrf2 signaling exacerbates oxidative stress-induced epithelial damage, whereas enhancement of Nrf2 activity confers resistance to oxidative insults in the gastrointestinal tract (31,32). In line with these reports, the present data demonstrated that H_2O_2 exposure suppressed nuclear Nrf2 accumulation and reduced HO-1 and NQO1 expression, whereas mulberroside A treatment was associated with concurrent increases in nuclear Nrf2 and downstream antioxidant proteins, aligning with improvements

in oxidative stress markers and barrier-associated parameters. The attenuation of these changes following Nrf2 knockdown further supports the association between Nrf2 signaling status and epithelial redox balance observed in previous studies (33,34).

Notably, the cell viability response to mulberroside A did not exhibit a strictly linear dose-response pattern. Mulberroside A alone caused only limited changes in basal Caco-2 cell viability across the tested concentrations, although higher concentrations tended to reduce viability. Similarly, in the H_2O_2-challenged model, the medium dose showed the greatest improvement in cell viability, whereas the high dose did not further enhance this effect. This may indicate that CCK-8-based viability, which mainly reflects cellular metabolic activity, does not necessarily parallel antioxidant and barrier-protective responses. By contrast, the effects of mulberroside A on ROS suppression and TEER restoration exhibited a clearer concentration-associated pattern.

The compound 2,3,5,4'-tetrahydroxystilbene-2-O-β-D-glycoside, a stilbene glycoside analogous to mulberroside A, has been shown to attenuate H_2O_2-induced oxidative damage in MC3T3-E1 osteoblasts in a dose-dependent manner through Nrf2/HO-1/NQO1 activation, with maximal effects at the highest dose tested (35). Mulberroside A itself has also been shown to inhibit oxidative stress in H_2O_2-stimulated Caco-2 cells, with higher doses conferring greater intestinal barrier protection (36). Thus, the enhanced ROS suppression and TEER restoration observed at 20 μM may reflect stronger activation of antioxidant responses involving the Nrf2/HO-1/NQO1 axis, strengthening antioxidant defense and tight junction preservation at higher concentrations.

The present study identified mulberroside A as a previously underexplored modulator of oxidative stress-associated intestinal epithelial barrier impairment. Using an established Caco-2 cell-based model, the present study showed that mulberroside A treatment under oxidative stress conditions was associated with concurrent alterations in Nrf2 nuclear accumulation, downstream antioxidant gene expression (HO-1 and NQO1), intracellular redox status and epithelial barrier integrity. Notably, genetic silencing of Nrf2 partially attenuated the protective effects of mulberroside A, supporting the involvement of Nrf2 signaling in mediating these cellular responses rather than solely representing a parallel event. By integrating molecular indicators of antioxidant signaling with biochemical measurements of oxidative stress, functional assessment of transepithelial resistance and structural evaluation of tight junction proteins, the present findings provide a multilevel view associating intracellular redox regulation with epithelial barrier preservation. Collectively, these findings extend current knowledge of mulberroside A beyond its reported antioxidant properties in non-intestinal tissues and offer mechanistic insights into its potential relevance in oxidative stress-associated intestinal epithelial injury, with possible implications for conditions such as inflammatory bowel disease (36,37).

The present study was performed in a Caco-2 cell-based *in vitro* model and further validation in animal models and *in vivo* systems is required to establish the physiological importance of the findings. In addition, epithelial barrier integrity was assessed mainly by TEER measurement and immunofluorescence staining of ZO-1 and occludin; therefore, additional western blotting validation of these tight junction proteins would further strengthen the protein-level evidence. Furthermore, as a glycoside, mulberroside A may undergo hydrolysis by intestinal microflora to its aglycone oxyresveratrol, potentially affecting its oral bioavailability; future pharmacokinetic studies are needed to clarify its *in vivo* absorption characteristics. Despite activation of Nrf2 signaling being closely associated with the observed effects of mulberroside A, the upstream regulatory mechanisms responsible for Nrf2 activation were not examined and require further investigation, particularly with regard to kelch-like ECH-associated protein 1-related regulation. In addition, the H_2O_2 model primarily represents acute oxidative stress and the impact of mulberroside A under chronic inflammatory or disease-relevant conditions remains to be determined. In addition, the present study focused primarily on nuclear Nrf2 levels; cytoplasmic and total Nrf2 protein data would provide a more complete view of Nrf2 nuclear translocation dynamics and warrants examination in future investigations. Collectively, the present findings provide a mechanistic basis for subsequent studies aimed at elucidating the function of mulberroside A in oxidative stress-associated intestinal disorders.

In conclusion, the present results indicated that mulberroside A attenuated oxidative stress-induced intestinal epithelial barrier dysfunction in Caco-2 cells, accompanied by reduced oxidative stress and preservation of tight junction integrity. These effects were closely associated with activation of the Nrf2/HO-1 antioxidant pathway, as supported by increased Nrf2 nuclear accumulation and downstream antioxidant responses. Collectively, these findings provided mechanistic insight into the intestinal protective potential of mulberroside A and thus support further investigation of mulberroside A in oxidative stress-associated intestinal epithelial injury.

Acknowledgements

Not applicable.

Funding

No funding was received.

Availability of data and materials

The data generated in the present study may be requested from the corresponding author.

Authors' contributions

JC, XH and XC conceived and designed the study. JC and WJ performed the experiments and collected the data. DL conducted the statistical analyses and interpreted the results. XH and XC supervised the project and revised it critically for important intellectual content. JC drafted the manuscript. All authors read and approved the final version of the manuscript. JC and XH confirm the authenticity of all the raw data.

Ethics approval and consent to participate

Not applicable.

Patient consent for publication

Not applicable.

Competing interests

The authors declare that they have no competing interests.

References

1. Wang R, Li Z, Liu S and Zhang D: Global, regional and national burden of inflammatory bowel disease in 204 countries and territories from 1990 to 2019: A systematic analysis based on the Global Burden of disease study 2019. BMJ Open 13: e065186, 2023.
2. Kaplan GG: The global burden of inflammatory bowel disease: From 2025 to 2045. Nat Rev Gastroenterol Hepatol 22: 708-720, 2025.
3. Arumugam P, Saha K and Nighot P: Intestinal epithelial tight junction barrier regulation by novel pathways. Inflamm Bowel Dis 31: 259-271, 2024.
4. Muro P, Zhang L, Li S, Zhao Z, Jin T, Mao F and Mao Z: The emerging role of oxidative stress in inflammatory bowel disease. Front Endocrinol (Lausanne) 15: 1390351, 2024.
5. Jin J, Cen T, Huang M, Xu F, Ding Q, Lv D, Wang S, Fei L, Ma H and Fu P: Involvement of mitochondrial unfolded protein response and activating transcription factor 4 in the mitochondrial damage pathway of BEAS-2B cells induced by cigarette smoke extracts. J Thorac Dis 17: 9586-9597, 2025.
6. Kustra A, Maliszewska-Olejniczak K, Sekrecka-Belniak A, Kulawiak B and Bednarczyk P: Polystyrene nanoplastics in human gastrointestinal Models-cellular and molecular mechanisms of toxicity. Int J Mol Sci 26: 11738, 2025.
7. Tratenšek A, Locatelli I, Grabnar I, Drobne D and Vovk T: Oxidative stress-related biomarkers as promising indicators of inflammatory bowel disease activity: A systematic review and meta-analysis. Redox Biol 77: 103380, 2024.
8. Rodrigues Junior JI, Vasconcelos JKG, Xavier LEMDS, Gomes ADS, Santos JCF, Campos SBG, Martins ASDP, Goulart MOF and Moura FA: Antioxidant therapy in inflammatory bowel disease: A systematic review and a Meta-analysis of randomized clinical trials. Pharmaceuticals (Basel) 16: 1374, 2023.
9. Bora SJ, Bhattacharyya S, Deb S and Sarkar D: Phytochemicals as potential therapeutic agents for inflammatory bowel disease: A comprehensive review. Phytochem Rev 25: 1985-2026, 2026.
10. Paudel D, Nair DVT, Joseph G, Castro R, Tiwari AK and Singh V: Gastrointestinal microbiota-directed nutritional and therapeutic interventions for inflammatory bowel disease: Opportunities and challenges. Gastroenterol Rep (Oxf) 12: goae033, 2024.
11. Wang X, Cheng Y, Huang J, Xu F, Jiang J, Nalinratana N, Jin L and Xue Y: Engineered probiotics for inflammatory bowel disease therapy: Mechanisms, delivery strategies, and precision medicine. Front Microbiol 16: 1696524, 2025.
12. Yuan L, Wang Y, Li N, Yang X, Sun X, Tian H and Zhang Y: Mechanism of action and therapeutic implications of Nrf2/HO-1 in inflammatory bowel disease. Antioxidants (Basel) 13: 1012, 2024.
13. Khan MZ, Li S, Ullah A, Li Y, Abohashrh M, Alzahrani FM, Alzahrani KJ, Alsharif KF, Wang C and Ma Q: Therapeutic agents targeting the Nrf2 signaling pathway to combat oxidative stress and intestinal inflammation in veterinary and translational medicine. Vet Sci 13: 25, 2025.
14. Chen H, Li Y, Wang J, Zheng T, Wu C, Cui M, Feng Y, Ye H, Dong Z and Dang Y: Plant polyphenols attenuate DSS-induced ulcerative colitis in mice via antioxidation, anti-inflammation and microbiota regulation. Int J Mol Sci 24: 10828, 2023.
15. Wallner M, Stadlbauer V, Blank-Landeshammer B, Heckmann M, Sadova N, Iken M, Pitari GM and Weghuber J: Plant extracts identified by in vitro high-content screening improve epithelial barrier function and attenuate oxidative and inflammatory stress. Pharmacol Res Nat Prod 7: 100226, 2025.
16. Li J, Wang J, Li Y, Guo J, Jin Z, Qiao S, Zhang Y, Li G, Liu H and Wu C: Mulberroside A: A Multi-target neuroprotective agent in Alzheimer's disease via cholinergic restoration and PI3K/AKT pathway activation. Biology (Basel) 14: 1114, 2025.
17. Liu T, Zhang Q, Zhao F, Yin J, Liu H, Wang L and Liu B: Mulberroside A alleviates myocardial infarction by inhibiting oxidative stress and apoptosis via the PI3K/Akt signaling pathway. Bratislava Med J 126: 2148-2156, 2025.
18. Shi B, Qian J, Miao H, Zhang S, Hu Y, Liu P and Xu L: Mulberroside A ameliorates CCl4-induced liver fibrosis in mice via inhibiting pro-inflammatory response. Food Sci Nutr 11: 3433-3441, 2023.
19. Liu Y, Chen M, Chen C and Huang G: In vitro and in vivo investigation of the capacity of mulberroside A to inhibit senescence. NPJ Sci Food 9: 198, 2025.
20. Donetti E, Bendinelli P, Correnti M, Gammella E, Recalcati S and Ferraretto A: Caco2/HT-29 in vitro cell Co-Culture: Barrier integrity, permeability, and tight Junctions' composition during progressive passages of parental cells. Biology (Basel) 14: 267, 2025.
21. Dong Y, Hou Q, Lei J, Wolf PG, Ayansola H and Zhang B: Quercetin alleviates intestinal oxidative damage induced by H2O2 via modulation of GSH: In vitro screening and in vivo evaluation in a colitis model of mice. ACS Omega 5: 8334-8346, 2020.
22. Hasegawa T, Mizugaki A, Inoue Y, Kato H and Murakami H: Cystine reduces tight junction permeability and intestinal inflammation induced by oxidative stress in Caco-2 cells. Amino Acids 53: 1021-1032, 2021.
23. Livak KJ and Schmittgen TD: Analysis of relative gene expression data using real-time quantitative PCR and the 2(-Delta Delta C(T)) method. Methods 25: 402-408, 2001.
24. Shen C, Luo Z, Ma S, Yu C, Lai T, Tang S, Zhang H, Zhang J, Xu W and Xu J: Microbe-derived antioxidants protect IPEC-1 cells from H2O2-induced oxidative stress, inflammation and tight junction protein disruption via activating the Nrf2 pathway to inhibit the ROS/NLRP3/IL-1β signaling pathway. Antioxidants (Basel) 13: 533, 2024.
25. Chen L, Chu H, Hu L, Li Z, Yang L and Hou X: The role of NADPH oxidase 1 in alcohol-induced oxidative stress injury of intestinal epithelial cells. Cell Biol Toxicol 39: 2345-2364, 2023.
26. Lin PY, Stern A, Peng HH, Chen JH and Yang HC: Redox and metabolic regulation of intestinal barrier function and associated disorders. Int J Mol Sci 23: 14463, 2022.
27. Li G, Wang S and Fan Z: Oxidative stress in intestinal Ischemia-reperfusion. Front Med (Lausanne) 8: 750731, 2021.
28. Stojanovic B, Milivojcevic Bevc I, Dimitrijevic Stojanovic M, Stojanovic BS, Jovanovic M, Lazarevic S, Milosevic B, Radosavljevic I, Tasic-Uros D, Markovic N, *et al*: Nrf2 as a molecular guardian of redox balance and barrier integrity in IBD. Antioxidants (Basel) 14: 1407, 2025.
29. Peng S, Shen L, Yu X, Zhang L, Xu K, Xia Y, Zha L, Wu J and Luo H: The role of Nrf2 in the pathogenesis and treatment of ulcerative colitis. Front Immunol 14: 1200111, 2023.
30. Shuhua Y, Lingqi M, Yunlong D, He T, Yao S and Peng L: Proanthocyanidins activate Nrf2/ARE signaling pathway in intestinal epithelial cells by inhibiting the ubiquitinated degradation of Nrf2. Biomed Res Int 2022: 8562795, 2022.
31. Yang Y, Chai H, Lan T, Gan Q, Liang Y, Tang C, Zeng Y and Liang H: SMP30 May protect human lens epithelial cells against high glucose-induced oxidative damage by regulating the Keap1/Nrf2/NQO1 pathway. Sci Rep 15: 43233, 2025.
32. Shi M, Luan Y, Zhang Z, Xi X and Li W: FSTL1 silencing protects against lipopolysaccharide-induced ferroptosis in renal tubular cells by regulating the PI3K/Akt pathway. Peptides 194: 171454, 2025.
33. Chen C, Tao M, Wang L, Yan W, Lin R and Fu Y: Nicotinamide N-methyltransferase mediates redox regulation and colonic epithelial barrier impairment by SIRT1/PPAR-γ/NLRP6/NRF2 axis in inflammatory bowel disease. Int Immunopharmacol 168: 115882, 2026.
34. Lim HS, Park J, Whang WJ, Kang WS, Kim S, Yoo YS and Park G: Melatonin ameliorates desiccation Stress-induced ocular inflammation in an in vitro model by activating the Nrf2 pathway. J Cell Mol Med 29: e70879, 2025.
35. Cheng J, Wang H, Zhang Z and Liang K: Stilbene glycoside protects osteoblasts against oxidative damage via Nrf2/HO-1 and NF-κB signaling pathways. Arch Med Sci 15: 196-203, 2019.
36. Yu R, Wen S, Wang Q, Wang C, Zhang L, Wu X, Li J and Kong L: Mulberroside A repairs high fructose diet-induced damage of intestinal epithelial and blood-brain barriers in mice: A potential for preventing hippocampal neuroinflammatory injury. J Neurochem 157: 1979-1991, 2021.
37. Wang M, Hu X and Xiong S: Pharmacological activities and pharmacokinetic properties of mulberroside: A systematical review. Fitoterapia 186: 106799, 2025.